INFECTION AND IMMUNITY, Nov. 2001, p. 6785–6795 Vol. 69, No. 11
0019-9567/01/$04.00+0 DOI: 10.1128/IAI.69.11.6785–6795.2001

Type III Secretion-Dependent Cell Cycle Block Caused in HeLa Cells by Enteropathogenic *Escherichia coli* O103

JEAN-PHILIPPE NOUGAYRÈDE,* MICHÈLE BOURY, CHRISTIAN TASCA, OLIVIER MARCHÈS, ALAIN MILON, ERIC OSWALD, AND JEAN DE RYCKE

UMR 960 de Microbiologie Moléculaire, Institut National de la Recherche Agronomique-Ecole Nationale Vétérinaire de Toulouse, 31076 Toulouse Cedex, France

Received 21 February 2001/Returned for modification 30 May 2001/Accepted 3 August 2001

Rabbit enteropathogenic *Escherichia coli* (EPEC) O103 induces in HeLa cells an irreversible cytopathic effect characterized by the recruitment of focal adhesions, formation of stress fibers, and inhibition of cell proliferation. We have characterized the modalities of the proliferation arrest and investigated its underlying mechanisms. We found that HeLa cells that were exposed to the rabbit EPEC O103 strain E22 progressively accumulated at 4C DNA content and did not enter mitosis. A significant proportion of the cells were able to reinitiate DNA synthesis without division, leading to 8C DNA content. This cell cycle inhibition by E22 was abrogated in mutants lacking EspA, -B, and -D and was restored by transcomplementation. In contrast, intimin and Tir mutants retained the antiproliferative effect. The cell cycle arrest was not a direct consequence of the formation of stress fibers, since their disruption by toxins during exposure to E22 did not reverse the cell cycle inhibition. Likewise, the cell cycle arrest was not dependent on the early tyrosine dephosphorylation events triggered by E22 in the cells. Two key partner effectors controlling entry into mitosis were also investigated: cyclin B1 and the associated cyclin-dependent kinase 1 (Cdk1). Whereas cyclin B1 was not detectably affected in E22-exposed cells, Cdk1 was maintained in a tyrosine-phosphorylated inactive state and lost its affinity for p13^{suc1}-agarose beads. This shows that Cdk1 is implicated in the G_2/M arrest caused by EPEC strain E22.

Enteropathogenic *Escherichia coli* (EPEC) constitutes a major cause of severe diarrheal disease in infants of the developing world (33). EPEC bacteria colonize the intestinal mucosa and produce specific attaching-and-effacing (A/E) lesions on gut enterocytes, characterized by intimate bacterial adhesion, formation of gross cytoskeletal structures beneath intimately attached bacteria, and destruction of the brush border microvilli (32). The intimate adhesion is considered to play a central role in EPEC-mediated disease, but the mechanisms by which EPEC causes diarrhea remains poorly characterized.

In the human reference EPEC strain E2348/69, the determinants of A/E lesions are encoded within a 35-kb chromosomal pathogenicity island, the locus of enterocyte effacement (LEE) (30). Similar pathogenicity islands are present in rabbit EPEC O103, in rabbit EPEC O15 strain RDEC-1, in enterohemorrhagic *E. coli*, and in other A/E pathogens (10, 14). The LEE encodes a type III secretion system homologous to those found in other pathogens, dedicated to the secretion and translocation of pathogenicity-associated proteins (20, 28). At least five proteins are secreted via this type III machinery, namely, EspA, -B, -D, and -F and Tir (21–23, 27, 31). EspA forms appendages that link the bacteria to target cells to allow the translocation of EspB and Tir into host cells (23, 25, 49). Recent experimental data suggest that EspB and EspD might be inserted in the target cell membrane to function as translocators for effector proteins (26, 46, 48, 49). In addition, EspB is found in the cytoplasm of exposed cells, and when transiently expressed in cultured cells it promotes actin rearrangements (44, 49). Once inserted in the target cell membrane, Tir serves as a receptor for an EPEC outer membrane protein, intimin (23, 40). This interaction leads to the local rearrangement of the cytoskeleton together with intimate adhesion of the bacterium on the host cell.

In addition to intimate adhesion, EPEC bacteria also modulate signaling pathways within cultured cells. EPEC bacteria activate protein kinase C and alter the phosphorylation state of several host proteins (14). Tyrosine dephosphorylation of several unidentified host proteins was correlated with the inhibition of phagocytosis by cultured macrophage cells (24, 15). Tyrosine phosphorylation of phospholipase C-γ1 and induction of inositol triphosphate and Ca^{2+} fluxes have been described, but increased intracellular Ca^{2+} is not required for A/E lesion formation (14, 24). EPEC increases paracellular permeability and stimulates ion secretion (7, 41). The integration of the A/E lesion and host cell responses in the induction of diarrhea is not fully elucidated.

We have previously shown that rabbit EPEC O103, the rabbit EPEC O15 strain RDEC-1, and certain human clinical EPEC isolates, but not the human reference EPEC strain E2348/69, trigger in HeLa cells an irreversible cytopathic effect (CPE). The CPE is characterized by the progressive recruitment of focal adhesions and assembly of stress fibers (10, 35). The cytoskeletal alterations are associated with an arrest of cell proliferation, as assessed by the inhibition of protein synthesis (10). The CPE is not reproducible by using supernatants or concentrated sonicates of CPE-positive EPEC strains, nor is it attributable to cytotoxic necrotizing factor, a toxin known to also cause the irreversible formation of actin stress fibers (10, 36). The triggering of the cytoskeletal alterations depends on a functional EPEC type III secretion machinery and requires EspA, -B, and -D but not Tir or intimin (10, 29, 35). No single

* Corresponding author. Present address: Division of Infectious Diseases, University of Maryland at Baltimore, 10 S. Pine St., Baltimore, MD 21201. Phone: (410) 706-7560. Fax: (410) 706-8700. E-mail: jnoug001@umaryland.edu.

TABLE 1. EPEC strains used in this study

Strain	Description (reference)
E2348/69	Prototype O127:H6 human EPEC strain
E22	Prototype rabbit EPEC O103:K-:H2, rhamnose-negative strain (10)
E22ΔEae	E22 *eae*::*aphT*, nonpolar Eae$^-$ mutant (35)
E22ΔTir	E22 *tir*::*aphT*, nonpolar Tir$^-$ mutant (29)
E22ΔEspA	E22 *espA*::*aphT*, nonpolar EspA$^-$ mutant (35)
E22ΔEspB	E22 *espB*::*aphT*, nonpolar EspB$^-$ mutant (35)
E22ΔEspD	E22 *espD*::*aphT*, nonpolar EspD$^-$ mutant (35)
E22ΔEspA(pBRespA$_{EPEC}$)	E22ΔEspA transformed with *espA* from E2348/69 cloned into pBRSK vector (35)
E22ΔEspB(pBRespB$_{EPEC}$)	E22ΔEspB transformed with *espB* from E2348/69 cloned into pBRSK vector (35)
E22ΔEspD(pBRespD$_{EPEC}$)	E22ΔEspD transformed with *espD* from E2348/69 cloned into pBRSK vector (35)

espA, *espB*, or *espD* gene encodes the specific information needed to trigger the cytoskeletal rearrangements, since each *espA*, *espB*, or *espD* mutant is fully complemented by the corresponding *esp* gene cloned from CPE-negative E2348/69 (35).

In the present study, we have investigated in more detail the arrest of cell proliferation that is associated with the cytoskeletal rearrangements. We found that cells exposed to rabbit EPEC strain E22 irreversibly accumulated at 4C and 8C DNA content without entering mitosis. This effect was not functionally related to cytoskeletal rearrangement but was linked to the maintenance of the cyclin-dependent kinase Cdk1, a key effector driving entry into mitosis, in a premitotic, tyrosine-phosphorylated state.

MATERIALS AND METHODS

Bacteria and HeLa cell cultures. EPEC strains and their mutants are listed in Table 1. The E22 *espA, espB, espD, tir*, and *eae* mutants were shown to be nonpolar and are described elsewhere (29, 35). Before interaction with cell cultures, bacteria were grown at 37°C in Penassay broth (Difco) supplemented with appropriate antibiotics. HeLa cells (ATCC CCL2) were cultivated in Eagle's minimum essential medium (MEM) supplemented with 10% fetal calf serum (FCS) (Gibco), L-glutamine (200 mM), and gentamicin (40 μg/ml) at 37°C in a 5% CO_2 atmosphere. Synchronization of HeLa cells at the G_1/S border was carried out with nonconfluent cell cultures (10^6 cells in a 10-cm-diameter culture dish) by the double thymidine block method, and synchronization in prometaphase was achieved using nocodazole (100 nM for 16 h) (8). Type 1 cytolethal distending toxin (CDT-I) was prepared and added to the cells as described previously (8, 11). Labeling the cells with 5-bromo-2′-deoxyuridine (BrdU) (5 μg/ml; Boehringer) was achieved for 30 min or 6 h.

Interaction between HeLa cells and bacteria. This assay was described previously (10). Briefly, interactions were carried out in MEM buffered with 25 mM HEPES supplemented with 5% FCS and 1% mannose, with a starting inoculum of 10^3 bacteria per cell. At the end of the 4-h interaction period, the cells were washed four to six times with Earle balanced saline solution and fixed, or they were further incubated in MEM with 10% FCS and 200 μg of gentamicin/ml for 24, 48, or 72 h.

For stress fiber inhibition experiments, cells were preincubated for 2 h in the interaction medium in the presence of 1 μg of purified epidermal cell differentiation inhibitor (EDIN) (kindly provided by M. Sugai [43])/ml or a 1:100 dilution of a filtered sonic lysate of BL21(pDC3B) (a gift from P. Boquet) containing the DC3B chimeric toxin (3). Bacteria were then added and left in contact with cells for 4 h as described above. Control cells were pretreated with a lysate of BL21 without the plasmid.

For tyrosine phosphatase inhibition experiments, we used phenylarsine oxide (PAO) (1 μM; Calbiochem) or pervanadate (PV). PV was freshly made by mixing hydrogen peroxide (1 μl of 30% stock) with 25 μl of 500 mM sodium vanadate (Na_3VO_4) (Sigma) in 424 μl of phosphate-buffered saline (pH 7.4). The remaining hydrogen peroxide was removed by treatment with catalase (100 μg/ml) (Sigma). PV was added to the cells at a 1:1,000 dilution after 2 h of EPEC infection. Control cells were pretreated with the solution lacking sodium vanadate.

The trypan blue uptake assay was performed as already described (9). The lactate dehydrogenase (LDH) release assay was performed on HeLa cells in 96-well plates. After the interaction, the supernatant was collected and the LDH was quantified with the cytotoxicity kit from Roche Molecular Biochemicals, according to the manufacturer's recommendations.

Fluorescence microscopy. Microtubules were stained with rat anti-α-tubulin (clone YL1/2; Sera-lab) and fluorescein isothiocyanate (FITC)-conjugated rabbit anti-rat immunoglobulin G (IgG) antibodies (Vector) as already described (8). DNA was stained with diaminophenylindole (0.1 μg/ml; Molecular Probes). F-actin was labeled with rhodamine-phalloidin according to the manufacturer's instructions (Molecular Probes). Focal adhesions were demonstrated by labeling vinculin with anti-vinculin mouse monoclonal antibodies (clone VIN-11-5; Sigma) and FITC-conjugated anti-mouse IgG goat antiserum (Immunotech) as previously described (10). Slides were examined by fluorescence microscopy with a Leica microscope.

Flow cytometry analysis. The flow cytometry analysis of DNA and cyclin B1 content of HeLa cells was performed as described previously (8). Briefly, cells were trypsinized, fixed in 70% ethanol, permeabilized with 0.25% Triton X-100, and incubated with anti-cyclin B1 mouse monoclonal antibodies (clone GNS1; Pharmingen) followed by FITC-conjugated goat anti-mouse IgG (Sigma). Control experiments were achieved using an irrelevant isotypic mouse IgG (Immunotech). In the final step, cells were suspended in a DNA staining solution containing propidium iodide (10 μg/ml; Sigma) and RNase (1 mg/ml; Sigma) in phosphate-buffered saline.

Incorporated BrdU was labeled according to a procedure previously described (12), including a thermal denaturation of DNA at 100°C followed by indirect immunofluorescence using anti-BrdU mouse monoclonal antibodies (clone 3D4; Pharmingen) and FITC-conjugated goat anti-mouse IgG (Sigma). DNA staining was then performed as described above.

Flow cytometry analyses were performed on a FACScalibur flow cytometer (Becton Dickinson), using the red (630 nm) emission for DNA quantification and green (530 nm) for BrdU and cyclin B1 quantification. The data from at least 10^4 cells were collected and analyzed using CellQuest and ModFit softwares (Becton Dickinson). Cell aggregates were identified and removed from analysis by gating.

Western blotting analysis of phosphotyrosine proteins. HeLa cells lysis and immunoprecipitation of phosphotyrosine proteins were carried out using Triton X-100 as described elsewhere (24). Protein samples were resolved by sodium dodecyl sulfate–7% polyacrylamide gel electrophoresis (SDS–7% PAGE) and blotted onto Immobilon-P membranes, and tyrosine-phosphorylated proteins were revealed with antiphosphotyrosine monoclonal antibodies (clone 4G10; Upstate Biotechnology) followed by secondary goat anti-mouse IgG (Fab-specific)-peroxidase conjugate (Sigma) and then developed with the ECL chemiluminescence detection system (Amersham).

Demonstration of Cdk1 in E22-exposed cells. HeLa cells (5×10^5) were lysed in 100 μl of Laemmli buffer, and the samples (40 μg of proteins, from about 10^5 cells) were resolved by SDS–12% PAGE. Cdk1 was demonstrated by direct Western blotting using the PhosphoPlus cdc2(Tyr15) antibody kit (New England Biolabs) following the recommendations of the manufacturer. In other experiments, Cdk1 (Cdc2) was affinity purified using yeast p13^{suc1} and revealed as previously described (8, 45). Briefly, 2×10^6 cells were lysed in 300 μl of modified RIPA buffer, and Cdk1 was purified from 200 μg of total proteins by affinity to yeast recombinant p13^{suc1} -agarose (Upstate Biotechnology). Samples were resolved by SDS–12% PAGE and blotted onto Immobilon-P. The three isoforms of Cdk1 were demonstrated with rabbit anti-Cdk1 antibodies (Gibco) followed by secondary goat anti-rabbit IgG-peroxidase conjugate (Biosys). After stripping, the slow-migrating tyrosine-phosphorylated isoform of Cdk1 was revealed with 4G10 monoclonal antibodies as before.

Raw data of the blots were scanned with an Astra 1220S scanner (Umax), and

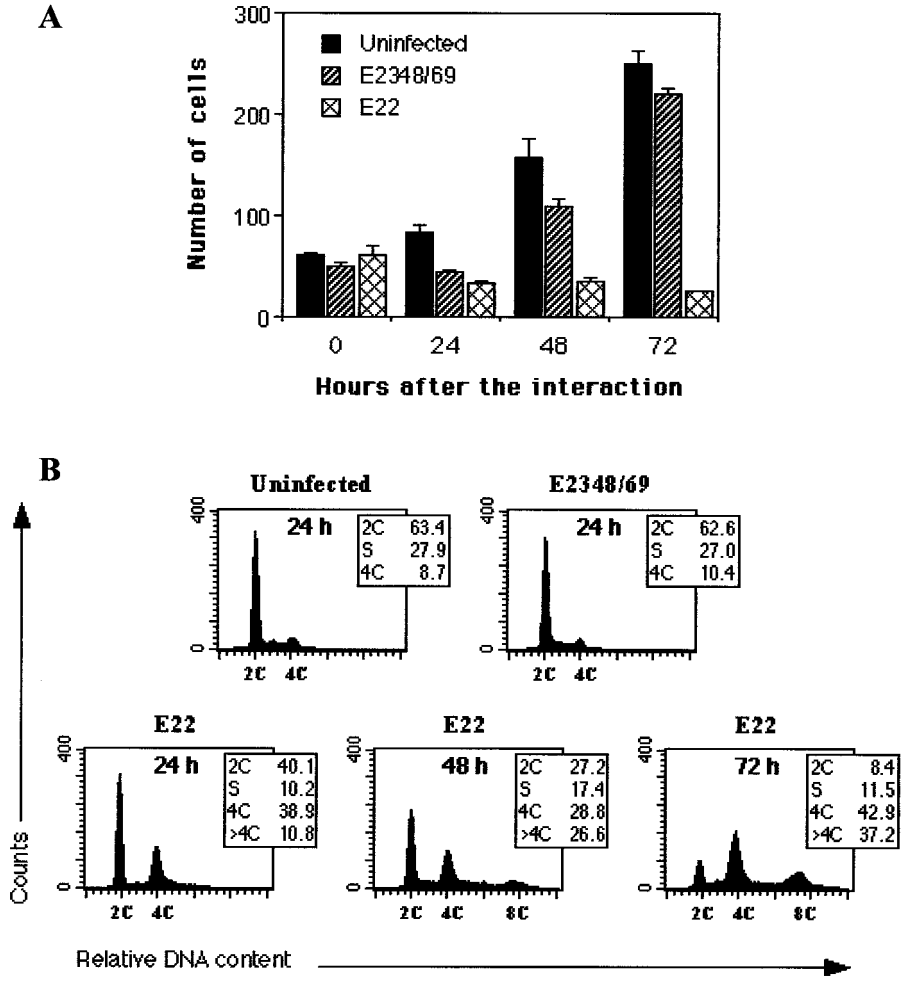

FIG. 1. Demonstration of the irreversible arrest in HeLa cell proliferation (A) and cell cycle perturbation (B) triggered by E22. Cells were exposed for 4 h to E2348/69 or E22 or left uninfected, and they were further cultivated for the indicated times. (A) Cell proliferation after interaction. Cultures were fixed and stained with Giemsa, and cells within random microscope fields were counted (objective, ×20). Each point is the mean of four independent measures. (B) Cell distribution according to DNA content, analyzed by flow cytometry after staining of DNA with propidium iodide. The percentages of cell populations are shown in each case.

the protein amount in each revealed band was estimated by densitometry, using National Institutes of Health image software (available at http://rsb.info.nih.gov/nih-image/).

RESULTS

EPEC strain E22 triggers an irreversible inhibition of mitosis. HeLa cells exposed to E22 for 4 h were irreversibly impaired in their proliferation, as assessed by cell counting (Fig. 1A). In contrast, cells exposed to E2348/69 were inhibited for about 24 h, after which their growth rate was similar to that of control cells (Fig. 1A). Morphologically, cells exposed to E22 progressively swelled and flattened, whereas cells exposed to E2348/69 behaved like control cells (data not shown), in agreement with previous observations (10).

This irreversible arrest in cell proliferation indicated that the cell cycle could be altered in a specific manner in E22-exposed cells. We thus analyzed the DNA content of cells exposed to E22 or E2348/69 by flow cytometry. The cell cycle distribution of cells exposed to E2348/69 was similar to that of control cells 24 h (Fig. 1B) or 48 to 72 h after the interaction (not shown). In contrast, cells exposed to E22 progressively accumulated in G_2/M (4C DNA content), while the number of cells in G_0/G_1 (2C DNA content) declined (Fig. 1B). In addition, a third peak at 8C DNA units was visible 72 h after the infection with E22 (Fig. 1B).

The foregoing results strongly suggested that the cells exposed to E22 were prevented from entering mitosis. In order to substantiate this result, DNA and α-tubulin were stained in E2348/69- or E22-exposed cells 24 h after the interaction. As shown by fluorescence microscopy, no figure of chromatin condensation (characteristic of prophase) or reorganization of microtubules into mitotic spindle was observed in E22-exposed cells (Fig. 2). These cells appeared mononucleated, and their nuclei were swollen (Fig. 2). In contrast, cells exposed to E2348/69 were actively dividing, showing typical mitotic spindle and figures of chromatin condensation (Fig. 2). For both E22- and E2348/69-exposed cells, these observations were confirmed 48 and 72 h after the interaction (not shown).

E22-induced mitosis inhibition is EspA, -B, and -D dependent but Tir and intimin independent. Our previous works

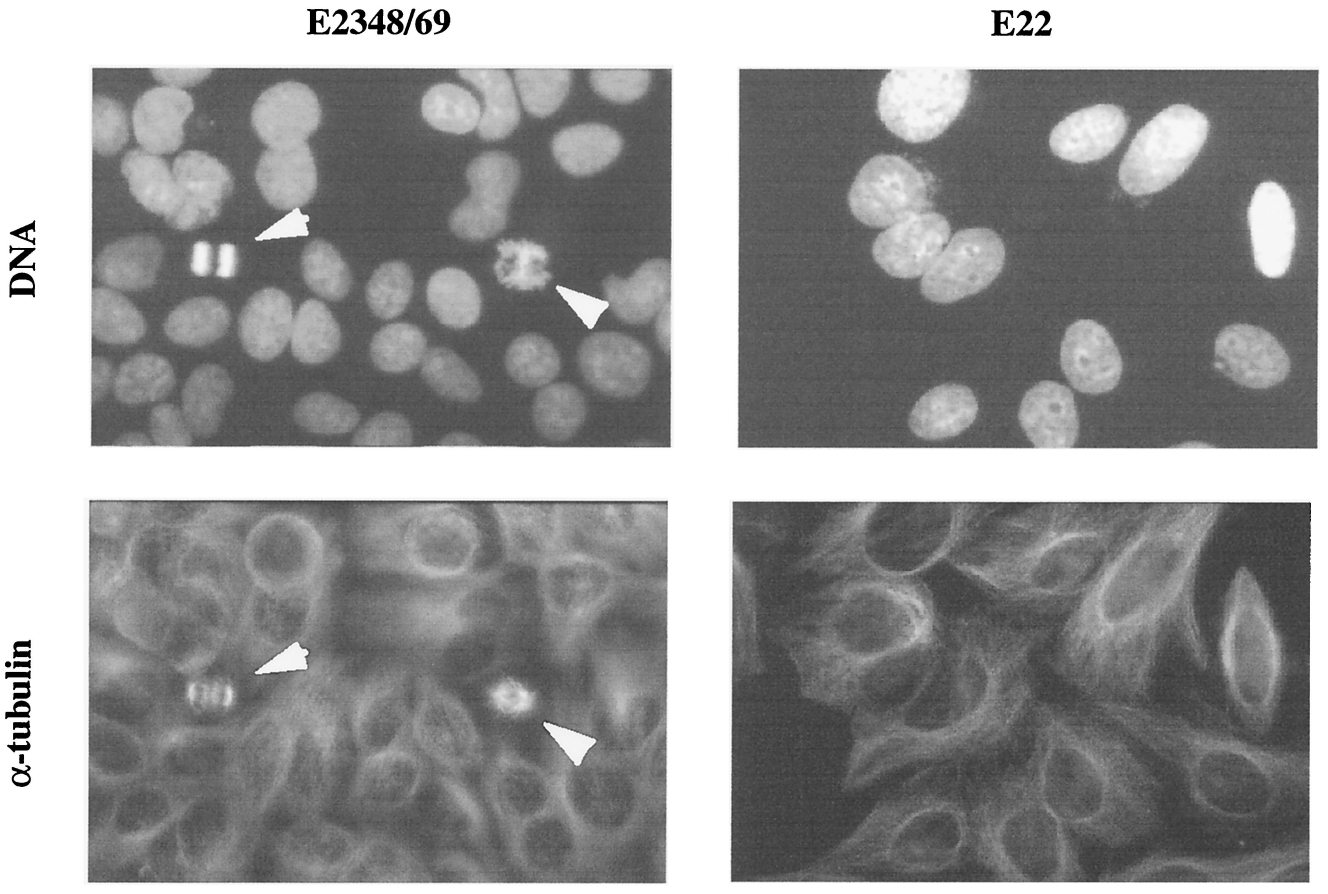

FIG. 2. Absence of mitotic figures in E22-exposed cells. Cells were exposed for 4 h to E2348/69 or E22 and further cultivated for 24 h. DNA was stained with diaminophenylindole, and α-tubulin was labeled by FITC indirect immunofluorescence. The same fields were photographed with a ×100 objective. Note the increased nuclear size in E22-exposed cells, compared to E2348/69-exposed cells, where figures of mitosis are visible (arrows).

indicate that the cytoskeletal rearrangement triggered by E22 in HeLa cells requires EspA, -B, and -D but not intimin and Tir (29, 35). We tested whether the antiproliferative effect of E22 follows the same pattern. The DNA content of HeLa cells exposed to E22 mutant strains was analyzed by flow cytometry 72 h after the interaction. Cells exposed to either E22ΔEae or E22ΔTir accumulated at 4C and 8C DNA content, whereas cells exposed to the nonpolar E22ΔEspA, E22ΔEspB, or E22ΔEspD mutant displayed a cell cycle distribution profile similar to that of uninfected control cells (Fig. 3). Cells exposed to each E22 *esp* mutant strain bearing in *trans* the corresponding *esp* gene cloned from E2348/69 accumulated at 4C and 8C DNA content (Fig. 3). In conclusion, the mitosis inhibition triggered by E22 was a process dependent on *espA*, *espB*, and *espD* but independent of *eae* and *tir*.

Dissociation of mitosis inhibition from cytoskeletal rearrangement. As shown above, the cytoskeletal rearrangement and the antiproliferative effect, both EspA, -B, and -D dependent and Tir/intimin independent, were phenotypically linked. Moreover, cell cycle perturbations may result from alterations of the cytoskeleton (2). We therefore reasoned that the cell cycle arrest could be a functional consequence of the cytoskeletal rearrangement and hence that the inhibition of stress fiber formation could possibly prevent the block. Since the cytoskeletal rearrangements are reminiscent of activated Rho (which plays a central role in stress fiber and focal adhesion assembly [39]), we attempted to inhibit stress fibers formation by inhibiting Rho before and during the interaction. To do so, we used *Clostridium botulinum* exoenzyme C3 and *Staphylococcus aureus* EDIN, two toxins that inhibit Rho. HeLa cells were pretreated for 2 h with either DC3B (a fusion protein of C3 and the B fragment of diphtheria toxin [3]) or purified EDIN (43), and then E22 was added and the interaction was prolonged for 4 h. After several washes, the cells were further cultivated without toxins and bacteria. Seventy-two hours after the interaction, cells exposed to E22 in absence of toxins exhibited the cytoskeleton alterations, namely, numerous stress fibers and clustered vinculin stretches (Fig. 4). In contrast, cells exposed to DC3B (or EDIN) and E22 were larger, rounder, and contained many fewer stress fibers, and vinculin was confined to the periphery of cells (Fig. 4 and data not shown). In control experiments, we verified that actin fibers were disrupted in HeLa cells treated with DC3B or EDIN at the expiration of the interaction period and that removal of toxins from the medium caused the recovery of actin fibers, vinculin structures, and cell growth (Fig. 4 and data not shown). In addition, DC3B and EDIN did not reduce HeLa cell viability (as assessed by the Trypan blue dye exclusion method and LDH assay) and did not impair E22 growth and adhesion (data not shown). The Rho inhibitors C3 and EDIN added before and during interaction

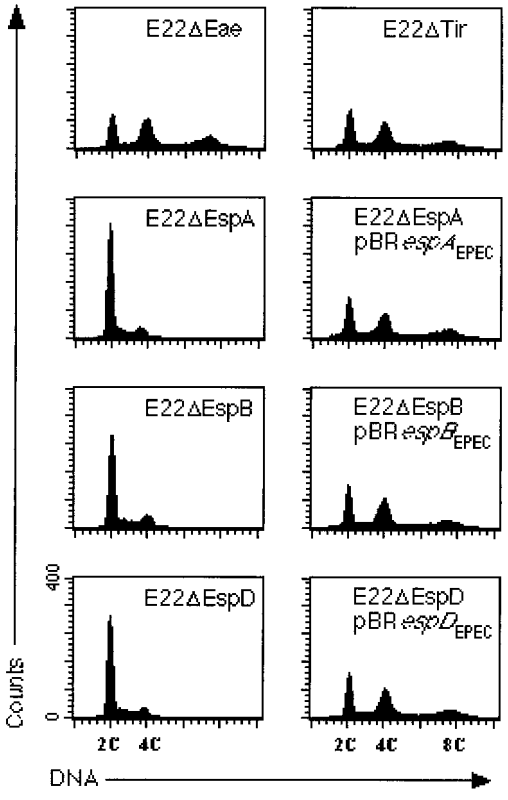

FIG. 3. Cell cycle patterns of HeLa cells 72 h after interaction with E22 mutant strains. The cell cycle arrest triggered by E22 required EspA, -B, and -D but neither intimin nor Tir. Each *esp* mutant was fully complemented by the corresponding *esp* gene cloned from E2348/69.

therefore efficiently prevented, in an irreversible manner, the cytoskeletal rearrangement triggered by E22.

This long-term disruption of stress fibers, however, did not prevent inhibition of mitosis. As shown by flow cytometry analysis, cells exposed to DC3B or EDIN and E22 and cultivated during 72 h accumulated at 4C and 8C (46.3 and 36.3%, respectively), a profile similar to that of cells exposed to E22 alone (43.3 and 36.5% at 4C and 8C, respectively) (Fig. 4 and data not shown). In contrast, the cell cycle distribution of cells exposed to DC3B or EDIN only was not significantly affected (Fig. 4 and data not shown). We can conclude that the antiproliferative effect was not functionally linked to cytoskeletal rearrangement.

Dissociation of mitosis inhibition from early tyrosine dephosphorylation events. Tyrosine dephosphorylation of several host cell proteins has been described as an early event induced by EPEC strain E2348/69 (24). E22-exposed HeLa cells exhibited a tyrosine dephosphorylation pattern similar to that induced by E2348/69, as demonstrated by immunoprecipitation and direct Western blotting of phosphotyrosine proteins (data not shown). Dephosphorylation events together with the 85- to 90-kDa phosphorylated Tir protein were detectable as early as 2 h after inoculation of cells with E22. The *espA*, *espB*, and *espD* mutants did not cause tyrosine dephosphorylation, which was restored after complementation by the corresponding gene cloned from E2348/69. In addition, *eae* and *tir* mutants induced a tyrosine dephosphorylation pattern similar to that in E22-exposed cells (data not shown).

Tyrosine kinase inhibitors are known to induce cell cycle arrest in several cell lines (6, 17). To determine whether the cytoskeletal rearrangement and the mitosis inhibition were dependent upon early tyrosine dephosphorylation,PV or PAO was used to inhibit tyrosine phosphatases during the interaction period. Cells were exposed to E22 for 2 h, and then the drug was added and the interaction was continued for 2 h. The overall tyrosine phosphorylation profile was even increased in PV- or PAO-treated cells compared to that of control cells (not shown). Seventy-two hours after the interaction, cells exposed to E22 in the presence of PAO or PV contained numerous stress fibers (data not shown) and a DNA content profile similar to that of cells exposed to E22 without the drugs (Fig. 5 and data not shown). Thus, the early tyrosine dephosphorylation events that occurred in E22-exposed cells were not necessary to the triggering of the mitosis inhibition and the cytoskeletal rearrangement.

Installation and maintenance of the G_2/M arrest in E22-exposed cells. With a view to investigating possible alterations induced by E22 infection in the biology of cellular effectors responsible for cell cycle progression, we analyzed more closely the modalities of the cell cycle arrest. The 8C peak demonstrated by cell cycle analysis indicates that cells blocked by E22, although not able to undergo mitosis, were able to enter a new round of DNA synthesis. In order to demonstrate DNA synthesis, HeLa cells were treated with BrdU for 6 h starting 72 h after initial exposure to E22 or E22ΔEspB, and then DNA and BrdU contents were quantified by flow cytometry. As shown in Fig. 6, 56.8 and 15.8% of E22ΔEspB-exposed cells were in G_0/G_1 and G_2/M, respectively, whereas 8.4, 42.9, and 15.2% of the cells exposed to E22 were identified in the G_0/G_1, G_2/M, and 8C populations, respectively. In E22ΔEspB-exposed cells, bivariate analysis showed that BrdU-labeled cells were present in S, G_2/M, and G_0/G_1 populations (Fig. 6), which demonstrated progression into a new cycle. In contrast, cells exposed to E22, although unable to enter a new G_1 phase, were able to incorporate BrdU after G_2/M phase, as illustrated by the presence of labeled cells in the 8C population (Fig. 6).

The foregoing results show that unsynchronized cells exposed to E22 progressively accumulated in G_2/M and 8C populations. To analyze more specifically the transition of cells through S to G_2 after the interaction, we exposed cells synchronized at the G_1/S border to E22 or E22ΔEspB. Thirty minutes or 24 h after the interaction period, cells were labeled with BrdU during 30 min and then processed for bivariate analysis by flow cytometry. One hour after the end of the interaction period (5 h after G_1/S release), 81.3% of the E22ΔEspB-infected cells had transited in S phase, as demonstrated by BrdU incorporation and DNA content (Fig. 7). At the same time, 74.2% of the E22-infected cells were also in S phase (Fig. 7). Twenty-four hours after the interaction, a majority of cells exposed to E22ΔEspB were distributed in G_0/G_1 and S phase (36.4 and 58.9%, respectively), which means that they were accomplishing a new cycle. In contrast, 70.5% of the cells exposed to E22 were in G_2/M, and 8.4% had greater than 4C DNA content (Fig. 7). In conclusion, cells exposed to E22 during S phase accumulated in G_2/M, and some of them rereplicated their DNA without intervening mitosis.

Expression of cyclin B1 in E22-exposed cells. Cdks associated with their regulatory units (cyclins) regulate progression

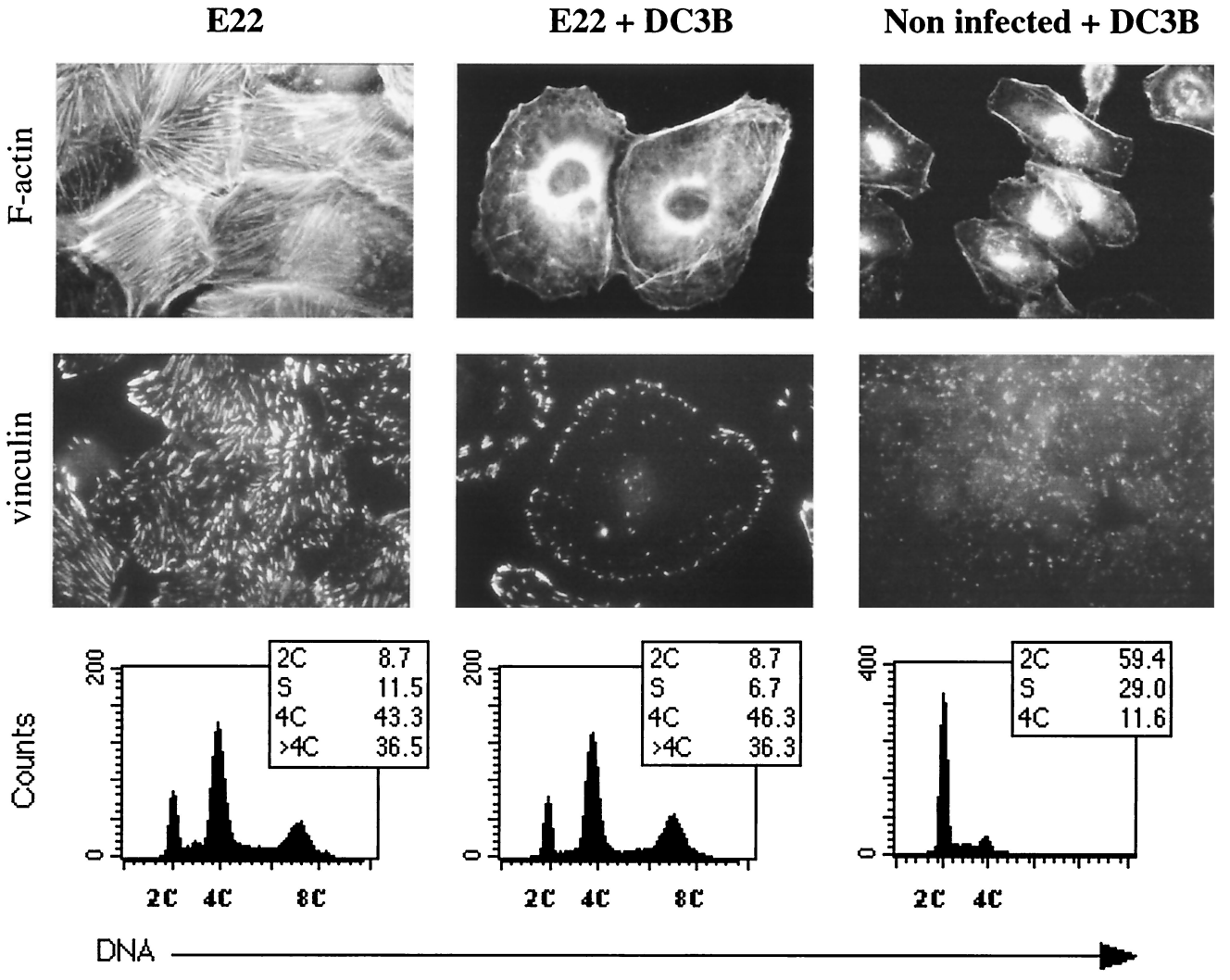

FIG. 4. Cytoskeletal rearrangement and cell distribution according to DNA content of HeLa cells 72 h after exposition to E22 in the presence or absence of the Rho inhibitor DC3B. HeLa cells were pretreated for 2 h with DC3B, and then E22 was added and the interaction was continued for 4 h. Control cells were treated with DC3B but left uninfected. After several washes, the cells were incubated for 72 h without bacteria and toxin. F-actin was stained with rhodamine-phalloidin, and vinculin was labeled by FITC indirect immunofluorescence. Corresponding cell distribution according to DNA content was determined by flow cytometry.

through the eukaryotic cell cycle. More specifically, cyclin B1 and Cdk1 control entry into mitosis. The cellular concentration of cyclin B1 is an immediate determinant of the transition from G_2 to mitosis (34). To test whether cyclin B1 expression was affected by exposition to E22, cells synchronized in G_1/S were infected as before, and the cyclin B1 concentration as a function of DNA content was determined by bivariate flow cytometry analysis. In cells exposed to E22ΔEspB, cyclin B1 accumulated during S phase (7 h after G_1/S release) and reached a maximum 11 h after G_1/S release (Fig. 8), when the majority of cells were in G_2 and about 5% were in mitosis (not shown). E22-exposed cells showed a similar cyclin B1 accumulation in S and G_2/M (Fig. 8). This indicated that cyclin B1 synthesis was not affected by exposition to E22 and prompted us to investigate Cdk1.

Cdk1 modification in E22-exposed cells. Cdk1 is expressed at a constant level over the different phases of the cell cycle, but its phosphorylation level increases during interphase to reach a maximum in G_2. Initiation of mitosis is then triggered by the activation of Cdk1, which results from dephosphorylation of the Tyr-15 residue (34). The amount of Cdk1 and its tyrosine phosphorylation status were determined in cells synchronized in G_1/S and exposed to bacteria as before. To validate the method, we used cells arrested in prometaphase by nocodazole (resulting in dephosphorylated active Cdk1) and cells blocked in G_2/M by treatment with CDT-I (resulting in hyperphosphorylated inactive Cdk1 [8]). The three isoforms of Cdk1 were demonstrated by direct Western blotting using anti-Cdk1 antibody (Fig. 9A and B), and after stripping of the membrane, antiphosphotyrosine antibodies were used to confirm that the slow-migrating Cdk1 isoform was tyrosine phosphorylated (not shown). As expected, the fast-migrating dephosphorylated isoform of Cdk1 was dominant in nocodazole-treated cells, while in CDT-I-treated cells the slow-migrating hyperphosphorylated isoform of Cdk1 was prevalent (Fig. 9A). In E22ΔEspB-exposed cells, the concentration of

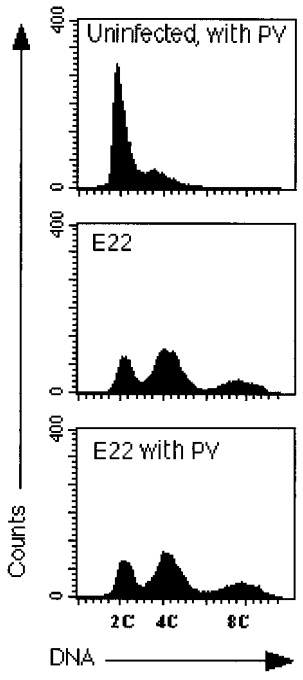

FIG. 5. Distribution of HeLa cells according to DNA content 72 h after the interaction in the presence or absence of the tyrosine phosphatase inhibitor PV. Cells were infected with E22 for 2 h, PV was added, and the interaction was continued for 2 h. After several washes, the cells were incubated for 72 h without bacteria and PV, and then the cell distribution according to DNA content was determined by flow cytometry.

the hyperphosphorylated upper isoform of Cdk1 was maximum in G_2 phase (11-h time point) and was lowered 24 h after the interaction (Fig. 9A; densitometry data not shown), consistent with the fact that these cells were accomplishing a new cycle (see Fig. 7). In E22-exposed cells, the concentration of the three isoforms of Cdk1 was similar to that of E22ΔEspB-exposed cells at the 7- and 11-h time points, but the concentration of hyperphosphorylated slow-migrating band remained high at the 24-h time point (Fig. 9A; densitometry data not shown), when about 70% of the cells were at 4C DNA content (Fig. 7). Thus, the kinetic of the accumulation of the cells at 4C DNA content was correlated to the hyperphosphorylation status of Cdk1, suggesting that the G_2/M arrest triggered by E22 is associated with the prevention of Cdk1 dephosphorylation.

p13^{suc1}, which binds Cdk1, is widely used as a reagent for precipitating Cdk1 from all eukaryotes (45). With a view to substantiate the foregoing result, Cdk1 was first affinity purified from cell lysates using p13^{suc1}-agarose beads before revelation by Western blotting. In E22ΔEspB-exposed cells, the total amount of the three isoforms of affinity-purified Cdk1 appeared similar in S phase and G_2 phase (11-h time point), while the hyperphosphorylated isoform increased to reach a maximum in G_2 (Fig. 9B). In comparison, in cells exposed to E22, the total amount of Cdk1 demonstrated by p13^{suc1} affinity was similar to that of E22ΔEspB-exposed cells 7 h after G_1/S release but about four times less abundant 11 h after release (Fig. 9B; densitometry data not shown). This reduction of Cdk1 affinity to p13^{suc1}-agarose beads was also observed 24 h after the interaction of E22 with unsynchronized cells (Fig. 9C). Taken together, these results indicate that the G_2/M arrest triggered by E22 is associated with the prevention of Cdk1 dephosphorylation and with the loss of Cdk1 affinity to exogenous p13^{suc1}.

DISCUSSION

Main features of the cell cycle arrest. This study sheds light on the modalities of the arrest of HeLa cell proliferation following exposure to strain E22 of the rabbit EPEC O103:H2 clonal group (10). The cytostatic effect triggered by E22 can be summarized as follows: cells progressively accumulate at 4C and 8C DNA content and do not display signs of mitosis during the whole period of observation, i.e., 72 h after the interaction. The kinetics of cell cycle distribution could suggest that unsynchronized cells exposed to E22 were arrested both in G_0/G_1 and in G_2/M (Fig. 1B). However, G_0/G_1 cells eventually transited to G_2/M, which suggests that G_1 cells were delayed and not stopped. Moreover, synchronized cells exposed in S phase accumulated in G_2/M without slowing down S-phase progression, which shows that G_2/M arrest was the major feature of the cell cycle perturbation (Fig. 7). It should be noticed that the capacity of a proportion of G_2/M-arrested cells to undergo a new round of DNA synthesis might result from a partial release in the mechanisms leading to the G_2/M arrest. This would give rise to tetraploid (8C) mononucleated cells that are unable to complete mitosis (Fig. 6). Such a phenomenon, called endoreduplication (16), has been observed with cell lines exposed to anticancer agents (47), the Simian virus 40 (42), or protein kinase inhibitors (17). We should also note that the HeLa cell genetic background could have influenced the occurrence of endoreduplication. Indeed, HeLa cells poorly express the inhibitor of Cdks p21$^{WAF1/CIP1}$ (19), which has an inhibitory effect on endoreduplication (47).

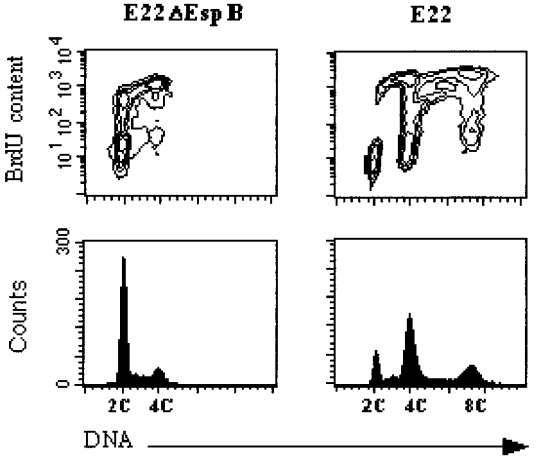

FIG. 6. Determination of BrdU incorporation in E22ΔEspB- and E22-exposed cells by bivariate flow cytometry. Seventy-two hours after exposition to bacteria, cells were treated for 6 h with BrdU (5 μg/ml). Incorporated BrdU was labeled by FITC indirect immunofluorescence, and DNA was labeled with propidium iodide. Contour maps of DNA red fluorescence versus FITC fluorescence are shown on the upper row, and corresponding DNA frequency distributions are displayed below.

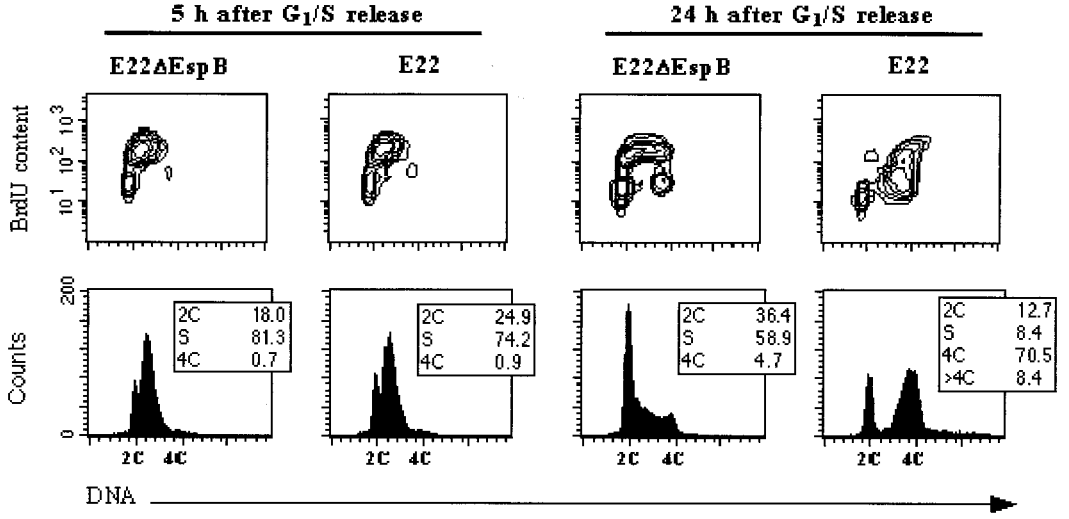

FIG. 7. Determination of BrdU incorporation in synchronized cells exposed to E22ΔEspB or E22. HeLa cells were synchronized at the G_1/S border and exposed for 4 h to bacteria at the time of release. Cells were treated for 30 min with BrdU (5 μg/ml) 5 or 24 h after release. Incorporated BrdU was labeled by FITC indirect immunofluorescence, and DNA was labeled by propidium iodide. Contour maps of DNA versus BrdU contents are on the upper row, and corresponding DNA frequency distributions are displayed below.

Bacterial effectors causing the G_2/M arrest. Certain traits of the cell cycle inhibition triggered by E22 are strikingly similar to that reported for cells exposed to CDTs. These toxins, which are produced by certain EPEC isolates (1), were shown to cause cell and nuclear distension and induce a G_2/M block through the maintenance of Cdk1 in hyperphosphorylated inactive state (8, 11). However, the participation of a toxin homologous to a CDT in E22-induced cell cycle arrest is unlikely, since no toxic activity could be detected in sterile lysates or in supernatants of E22 cultures (10), and we were unable to demonstrate homologous genes by degenerate PCR in rabbit EPEC O103 (unpublished data). In addition, the reduced affinity purification of Cdk1 by $p13^{suc1}$ in E22-exposed cells is not observed in CDT-treated cells (Fig. 9C) (8). Moreover, the triggering of cytoskeletal rearrangements together with cell proliferation arrest are dependent upon the type III secretion system (10), while CDT toxins do not rely upon type III secretion for delivery (38). We also demonstrate that the cell cycle arrest triggered by E22 is EspA, -B, and -D dependent but Tir and intimin independent (Fig. 3). Whether EspA, -B, and -D mediate cytoskeleton alterations and mitosis inhibition directly as effector proteins and/or indirectly as components of a translocation apparatus remains to be determined. However, each *espA*, *espB*, or *espD* mutant strain was functionally complemented by the corresponding *esp* gene cloned from the CPE-negative strain E2348/69, indicating that no single *espA*, *espB*, or *espD* gene encodes the information needed to confer the cytostatic capacity (Fig. 3) and the cytoskeleton alteration (35). Recent data support the notion that EspA, -B, and -D form a molecular syringe to allow the injection of effector molecules

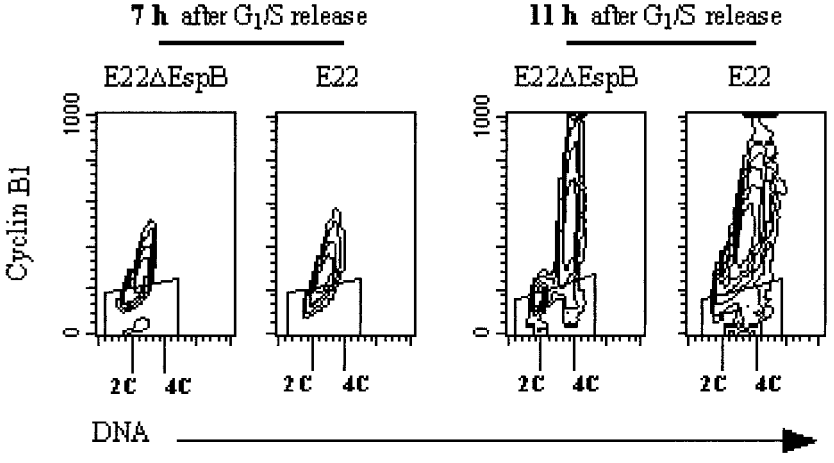

FIG. 8. Evolution of cyclin B1 content in synchronized cells exposed to E22 or E22ΔEspB. HeLa cells were synchronized at the G_1/S border and exposed for 4 h to bacteria starting at the time of release. The cells were harvested 7 and 11 h after release and processed for bivariate flow cytometry analysis. Cyclin B1 was labeled by FITC indirect immunofluorescence, and DNA was labeled by propidium iodide. Contour maps of cyclin B1 as a function of DNA content are shown. The "windows" represent the level of nonspecific fluorescence, i.e., fluorescence of the cells that were treated with irrelevant isotypic IgG rather than antibodies against cyclin.

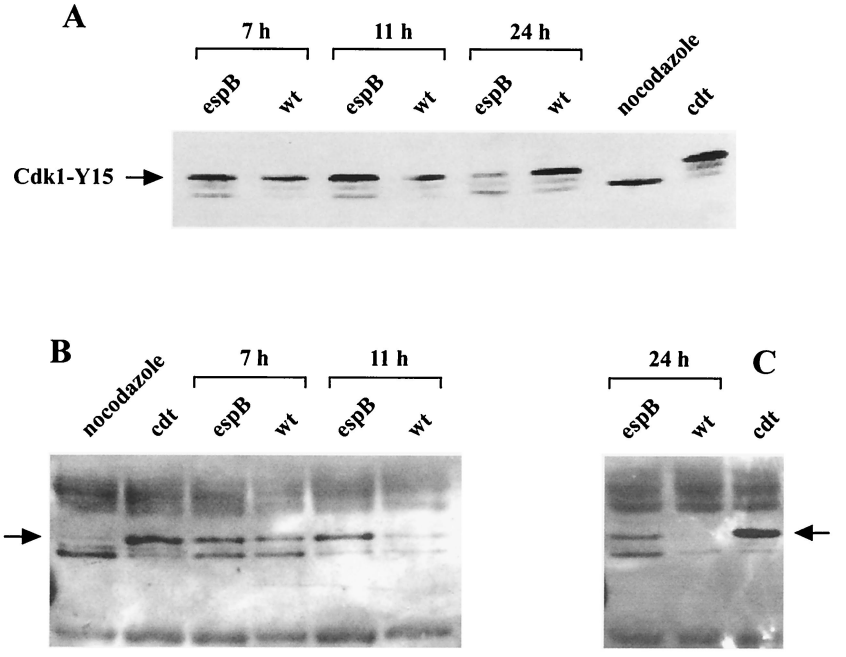

FIG. 9. Demonstration of Cdk1 in E22- and E22ΔEspB-exposed cells. HeLa cells synchronized at the G_1/S border (A and B) or left unsynchronized (C) were exposed to bacteria for 4 h and were harvested after 7, 11, and 24 h. (A) Cell lysates (40 μg of proteins from 5×10^5 cells) were resolved by SDS-PAGE, and the three isoforms of Cdk1 were revealed by Western blotting. (B and C) Cdk1 was affinity-purified from cell lysates (200 μg of proteins from 2×10^6 cells) using $p13^{suc1}$-agarose beads. After SDS-PAGE, the three isoforms of Cdk1 were revealed by Western blotting. Cells blocked in prometaphase by nocodazole (dephosphorylated Cdk1) and blocked in G_2/M by CDT-I (hyperphosphorylated Cdk1) were used as controls. The blots were stripped and reprobed with anti-Cdk1-Tyr15 or anti-phosphotyrosine antibodies to confirm that the slow-migrating isoform (noted by an arrow) was tyrosine phosphorylated (data not shown).

into the host cells by EPEC (25, 26, 48, 49). From all these data, we can hypothesize that the EPEC strain E22 produces at least one other factor that is specifically involved in CPE. This factor could depend on secreted EspA, -B, and -D for functionality and/or translocation. Alternatively, the Esps may trigger the cytoskeletal rearrangements and/or the mitosis inhibition, which are then altered by other factor(s) unique to each strain, eventually leading to the CPE phenotype. For instance, the negative strain E2348/69 may express an additional dominant determinant that prevents triggering of CPE.

Uncoupling of cell cycle arrest from cytoskeletal alteration. Correlation between the structure of the actin cytoskeleton and cell cycle progression have been reported: endoreduplication may result from alteration of the cytoskeleton (2), and the cytotoxic necrotizing toxins induce the formation of multinucleated cells containing numerous stress fibers and in parallel inhibit cell division (36). However, the inhibition of mitosis observed in this study is not likely to be a functional consequence of the cytoskeletal rearrangement triggered by E22, since the use of EDIN or C3 chimeric toxin DC3B efficiently prevented the multiplication of focal adhesions and stress fibers without impairing the cell cycle arrest (Fig. 4). Control cells treated with DC3B or EDIN alone showed a normal cytoskeleton and cell cycle pattern 72 h after treatment (Fig. 4), an observation consistent with the recently described reversal of C3 effects upon removal of the toxin from the medium (4). On the other hand, the irreversible inhibition of stress fiber assembly by DC3B in E22-exposed cells suggests that the small GTP-binding RhoA, the main target of DC3B, is crucial in the transduction cascade leading to the cytoskeleton rearrangement. Further works, for instance using Rho mutant cell lines, are needed to substantiate this hypothesis.

Cell cycle arrest and tyrosine dephosphorylation. Regulation of tyrosine phosphorylation represents a governing mechanism in cell proliferation (5). In certain cell systems, the protein kinase inhibitor staurosporine impairs cytokinesis and induces a higher DNA ploidy level (17). We therefore reasoned that the triggering of the cell cycle arrest by E22 could be preceded by the disruption of tyrosine phosphorylation events. E22 did induce an EspA, -B, and -D-dependent tyrosine dephosphorylation of host proteins. However, repressing the dephosphorylation induced by E22 with pervanadate or phenylarsine oxide impaired neither the cell cycle arrest nor the cytoskeletal rearrangement. In addition, the E22-induced phosphorylation profile was similar to that induced by E2348/69, a strain that is unable to trigger the cell cycle arrest. A recent work shows that E2348/69-induced tyrosine dephosphorylation events are linked to an antiphagocytic phenotype (15). Unpublished work done in our laboratory indicates that E22 also inhibits its entry in HeLa cells, an inhibition that depends on EspA, -B, and -D and which is impaired by pervanadate or phenylarsine oxide treatment. Thus, the detectable tyrosine dephosphorylation events that take place in the host cell following E22 exposition are related to an antiphagocytic activity exerted by EPEC on target cells but not to either cytoskeletal rearrangement or mitosis inhibition.

Implication of specific cellular effectors of the G_2-M transition. To investigate further the possible mechanisms of the G_2/M arrest triggered by E22, we have analyzed the behavior of the cyclin B1 and Cdk1, which form the complex controlling

the transition from G_2 to mitosis. In normal cells, cyclin B1 accumulates during S phase to reach a maximum in late G_2, whereas Cdk1 is present at a constant level over the different phases of the cell cycle. Cdk1 activity is downregulated by phosphorylation of Tyr-15 and Thr-14 residues, which remain phosphorylated during interphase until onset of M phase (34). The G_2/M arrest triggered by E22 could not be accounted for by a lack of cyclin B1 expression, since cyclin B1 expression was not affected in synchronous cells exposed to E22 (Fig. 8). On the other hand, we observed in E22-exposed synchronous cells an accumulation of inactive Cdk1 phosphorylated on Tyr-15 (Fig. 9A), in association with the accumulation of the cells at 4C DNA content (Fig. 7). Since Cdk1 dephosphorylation is a prerequisite for its activation and entry into mitosis, the lack of Cdk1 dephosphorylation may account for the G_2/M arrest. A further clue to the determinism of the cell cycle arrest triggered by E22 is provided by our observation that the G_2/M arrest was associated with a drastic reduction of the level of Cdk1 affinity purified with p13^{suc1}-agarose beads (Fig. 9B and C). p13^{suc1} is the founding member of the cyclin-dependent kinase subunit (Cks) family of proteins that bind and regulate Cdks, and it is widely used as a reagent for precipitating Cdk's from all eukaryotes (45). We can hypothesize that the binding of an endogenous Cks protein may have impaired binding of Cdk1 to p13^{suc1}-agarose beads. Indeed, overexpression of Cks abolishes entry into mitosis and causes an accumulation of inactive Cdk1 phosphorylated on Tyr-15 (13, 37). Alternatively, a putative Cdk1 alteration could alter its affinity to p13^{suc1} and participate in the cell cycle perturbation. The fact that certain cell cycle yeast mutants, carrying temperature-sensitive Cdk alleles, show a decrease in p13^{suc1}-bound Cdk without change in overall Cdk levels supports this idea (4a). The kinetics of association of Cdk1 with cyclin B1 and endogenous Cks together with their subcellular localization should now be assessed in order to explain the defect of exogenous p13^{suc1} affinity to Cdk1 and further unravel the alteration of cell cycle machinery in E22-exposed cells. Elucidation of the abnormal behavior of Cdk1 toward p13^{suc1} may provide a clue on upstream signaling events triggered upon E22 interaction and eventually preventing cell entry into mitosis.

Concluding remarks. The cell cycle arrest triggered by E22 appears to be relevant to other CPE-positive strains of the rabbit EPEC O103:H2 clonal group, rabbit EPEC O15 strain RDEC-1, and some human clinical EPEC isolates (10), since they had a similar effect on the HeLa cell cycle (data not shown). Is a modulation of the eukaryotic cell cycle relevant in EPEC pathogenesis? A cell cycle arrest of stem cells in the crypts of Lieberkhün, which supply cells to intestinal villi, could reduce the shedding of epithelia and therefore prolong the local existence of attached bacteria. In addition, the ability to inhibit proliferation could constitute a powerful weapon for immune evasion. There is emerging evidence that a growing family of pathogenic bacteria can subvert the eukaryotic cell cycle (18). Future work should hunt for a putative mitosis-inhibiting factor translocated into host cells by EPEC in an EspABD-dependent manner and should evaluate the impact of such a cell cycle modulation activity on the natural history of disease.

ACKNOWLEDGMENTS

We are indebted to M. Sugai for the kind gift of the purified EDIN and to P. Boquet for the gift of the plasmid encoding DC3B. We thank J. R. Seavitt, S. Boullier, and S. Pérès for useful advice, C. Watrin for technical assistance, and E. Blank for critical reading of the manuscript.

This work was supported by grants from the Région Midi-Pyrénées, from INRA (AIP Microbiologie), and from the DGER and by grant 1335 from the European Community Program FAIR. J.-P.N. was a recipient of a scholarship from INRA and Biové Company, and O.M. was a recipient of a scholarship from ENVT.

REFERENCES

1. **Albert, M. J., S. M. Faruque, A. S. Faruque, K. A. Bettelheim, P. K. Neogi, N. A. Bhuiyan, and J. B. Kaper.** 1996. Controlled study of cytolethal distending toxin-producing *Escherichia coli* infections in Bangladeshi children. J. Clin. Microbiol. **34:**717–719.
2. **Assoian, R. K., and X. Zhu.** 1997. Cell anchorage and the cytoskeleton as partners in growth factor dependent cell cycle progression. Curr. Opin. Cell Biol. **9:**93–98.
3. **Aullo, P., M. Giry, S. Olsnes, M. R. Popoff, C. Kocks, and P. Boquet.** 1993. A chimeric toxin to study the role of the 21 kDa GTP binding protein rho in the control of actin microfilament assembly. EMBO J. **12:**921–931.
4. **Barth, H., C. Olenik, P. Sehr, G. Schmidt, K. Aktories, and D. K. Meyer.** 1999. Neosynthesis and activation of rho by Escherichia coli cytotoxic necrotizing factor (CNF1) reverse cytopathic effects of ADP-ribosylated Rho. J. Biol. Chem. **274:**27407–27414.

4a. **Brizuela, L., G. Draetta, and Beach D.** 1987. p13suc1 acts in the fission yeast cell division cycle as a component of the p34cdc2 protein kinase. EMBO J. **6:**3507–3514.

5. **Chernoff, J.** 1999. Protein tyrosine phosphatases as negative regulators of mitogenic signaling. J. Cell. Physiol. **180:**173–181.
6. **Choi, Y. H., L. Zhang, W. H. Lee, and K. Y. Park.** 1998. Genistein-induced G_2/M arrest is associated with the inhibition of cyclin B1 and the induction of p21 in human breast carcinoma cells. Int. J. Oncol. **13:**391–396.
7. **Collington, G. K., I. W. Booth, and S. Knutton.** 1998. Rapid modulation of electrolyte transport in Caco-2 cell monolayers by enteropathogenic Escherichia coli (EPEC) infection. Gut **42:**200–207.
8. **Comayras, C., C. Tasca, S. Y. Peres, B. Ducommun, E. Oswald, and J. De Rycke.** 1997. Escherichia coli cytolethal distending toxin blocks the HeLa cell cycle at the G_2/M transition by preventing cdc2 protein kinase dephosphorylation and activation. Infect. Immun. **65:**5088–5095.
9. **Crane, J. K., S. Majumdar, and D. F. Pickhardt III.** 1999. Host cell death due to enteropathogenic Escherichia coli has features of apoptosis. Infect. Immun. **67:**2575–2584.
10. **De Rycke, J., E. Comtet, C. Chalareng, M. Boury, C. Tasca, and A. Milon.** 1997. Enteropathogenic Escherichia coli O103 from rabbit elicits actin stress fibers and focal adhesions in HeLa epithelial cells, cytopathic effects that are linked to an analog of the locus of enterocyte effacement. Infect. Immun. **65:**2555–2563.
11. **De Rycke, J., V. Sert, C. Comayras, and C. Tasca.** 2000. Sequence of lethal events in HeLa cells exposed to the G_2 blocking cytolethal distending toxin. Eur. J. Cell Biol. **79:**192–201.
12. **Dolbeare, F., and J. R. Selden.** 1994. Immunochemical quantitation of bromodeoxyuridine: application to cell-cycle kinetics. Methods Cell Biol. **41:** 297–316.
13. **Dunphy, W. G., and J. W. Newport.** 1989. Fission yeast p13 blocks mitotic activation and tyrosine dephosphorylation of the Xenopus cdc2 protein kinase. Cell **58:**181–191.
14. **Frankel, G., A. D. Phillips, I. Rosenshine, G. Dougan, J. B. Kaper, and S. Knutton.** 1998. Enteropathogenic and enterohaemorrhagic Escherichia coli: more subversive elements. Mol. Microbiol. **30:**911–921.
15. **Goosney, D. L., J. Celli, B. Kenny, and B. B. Finlay.** 1999. Enteropathogenic Escherichia coli inhibits phagocytosis. Infect. Immun. **67:**490–495.
16. **Grafi, G.** 1998. Cell cycle regulation of DNA replication: the endoreduplication perspective. Exp. Cell Res. **244:**372–378.
17. **Hall, L. L., J. P. Th'ng, X. W. Guo, R. L. Teplitz, and E. M. Bradbury.** 1996. A brief staurosporine treatment of mitotic cells triggers premature exit from mitosis and polyploid cell formation. Cancer Res. **56:**3551–3559.
18. **Henderson, B., M. Wilson, and J. Hyams.** 1998. Cellular microbiology: cycling into the millennium. Trends Cell Biol. **8:**384–387.
19. **Hwang, E. S., L. K. Naeger, and D. DiMaio.** 1996. Activation of the endogenous p53 growth inhibitory pathway in HeLa cervical carcinoma cells by expression of the bovine papillomavirus E2 gene. Oncogene **12:**795–803.
20. **Jarvis, K. G., J. A. Giron, A. E. Jerse, T. K. McDaniel, M. S. Donnenberg, and J. B. Kaper.** 1995. Enteropathogenic Escherichia coli contains a putative type III secretion system necessary for the export of proteins involved in attaching and effacing lesion formation. Proc. Natl. Acad. Sci. USA **92:**7996–8000.
21. **Kenny, B., and B. B. Finlay.** 1995. Protein secretion by enteropathogenic Escherichia coli is essential for transducing signals to epithelial cells. Proc.

Natl. Acad. Sci. USA **92:**7991–7995.
22. **Kenny, B., L. C. Lai, B. B. Finlay, and M. S. Donnenberg.** 1996. EspA, a protein secreted by enteropathogenic Escherichia coli, is required to induce signals in epithelial cells. Mol. Microbiol. **20:**313–323.
23. **Kenny, B., R. DeVinney, M. Stein, D. J. Reinscheid, E. A. Frey, and B. B. Finlay.** 1997. Enteropathogenic E. coli (EPEC) transfers its receptor for intimate adherence into mammalian cells. Cell **91:**511–520.
24. **Kenny, B., and B. B. Finlay.** 1997. Intimin-dependent binding of enteropathogenic Escherichia coli to host cells triggers novel signaling events, including tyrosine phosphorylation of phospholipase C-gamma1. Infect. Immun. **65:**2528–2536.
25. **Knutton, S., I. Rosenshine, M. J. Pallen, I. Nisan, B. C. Neves, C. Bain, C. Wolff, G. Dougan, and G. Frankel.** 1998. A novel EspA-associated surface organelle of enteropathogenic Escherichia coli involved in protein translocation into epithelial cells. EMBO J. **17:**2166–2176.
26. **Kresse, A. U., M. Rohde, and C. A. Guzman.** 1999. The EspD protein of enterohemorrhagic Escherichia coli is required for the formation of bacterial surface appendages and is incorporated in the cytoplasmic membranes of target cells. Infect. Immun. **67:**4834–4842.
27. **Lai, L. C., L. A. Wainwright, K. D. Stone, and M. S. Donnenberg.** 1997. A third secreted protein that is encoded by the enteropathogenic Escherichia coli pathogenicity island is required for transduction of signals and for attaching and effacing activities in host cells. Infect. Immun. **65:**2211–2217.
28. **Lee, C. A.** 1997. Type III secretion systems: machines to deliver bacterial proteins into eukaryotic cells? Trends Microbiol. **5:**148–156.
29. **Marches, O., J. P. Nougayrede, S. Boullier, J. Mainil, G. Charlier, I. Raymond, P. Pohl, M. Boury, J. De Rycke, A. Milon, and E. Oswald.** 2000. Role of Tir and intimin in the virulence of rabbit enteropathogenic Escherichia coli (REPEC) of serotype O103:H2. Infect. Immun. **68:**2171–2182.
30. **McDaniel, T. K., and J. B. Kaper.** 1997. A cloned pathogenicity island from enteropathogenic Escherichia coli confers the attaching and effacing phenotype on E. coli K-12. Mol. Microbiol. **23:**399–407.
31. **McNamara, B. P., and M. S. Donnenberg.** 1998. A novel proline-rich protein, EspF, is secreted from enteropathogenic Escherichia coli via the type III export pathway. FEMS Microbiol. Lett. **166:**71–78.
32. **Moon, H. W., S. C. Whipp, R. A. Argenzio, M. M. Levine, and R. A. Giannella.** 1983. Attaching and effacing activities of rabbit and human enteropathogenic Escherichia coli in pig and rabbit intestines. Infect. Immun. **41:** 1340–1351.
33. **Nataro, J. P., and J. B. Kaper.** 1998. Diarrheagenic Escherichia coli. Clin. Microbiol. Rev. **11:**142–201.
34. **Norbury, C., and P. Nurse.** 1992. Animal cell cycles and their control. Annu. Rev. Biochem. **61:**441–470.
35. **Nougayrede, J. P., O. Marches, M. Boury, J. Mainil, G. Charlier, P. Pohl, J. De Rycke, A. Milon, and E. Oswald.** 1999. The long-term cytoskeletal rearrangement induced by rabbit enteropathogenic Escherichia coli is Esp dependent but intimin independent. Mol. Microbiol. **31:**19–30.
36. **Oswald, E., M. Sugai, A. Labigne, H. C. Wu, C. Fiorentini, P. Boquet, and A. D. O'Brien.** 1994. Cytotoxic necrotizing factor type 2 produced by virulent Escherichia coli modifies the small GTP-binding proteins Rho involved in assembly of actin stress fibers. Proc. Natl. Acad. Sci. USA **91:**3814–3818.
37. **Patra, D., and W. G. Dunphy.** 1996. Xe-p9, a Xenopus Suc1/Cks homolog, has multiple essential roles in cell cycle control. Genes Dev. **10:**1503–1515.
38. **Pickett, C. L., and C. A. Whitehouse.** 1999. The cytolethal distending toxin family. Trends Microbiol. **7:**292–297.
39. **Ridley, A. J., and A. Hall.** 1992. The small GTP-binding protein rho regulates the assembly of focal adhesions and actin stress fibers in response to growth factors. Cell **70:**389–399.
40. **Rosenshine, I., S. Ruschkowski, M. Stein, D. J. Reinscheid, S. D. Mills, and B. B. Finlay.** 1996. A pathogenic bacterium triggers epithelial signals to form a functional bacterial receptor that mediates actin pseudopod formation. EMBO J. **15:**2613–2624.
41. **Savkovic, S. D., A. Koutsouris, and G. Hecht.** 1997. Activation of NF-kappaB in intestinal epithelial cells by enteropathogenic Escherichia coli. Am. J. Physiol. **273:**C1160–C1167.
42. **Scarano, F. J., J. A. Laffin, J. M. Lehman, and T. D. Friedrich.** 1994. Simian virus 40 prevents activation of M-phase-promoting factor during lytic infection. J. Virol. **68:**2355–2361.
43. **Sugai, M., K. Hashimoto, A. Kikuchi, S. Inoue, H. Okumura, K. Matsumoto, Y. Goto, H. Ohgai, K. Moriishi, B. Syuto, et al.** 1992. Epidermal cell differentiation inhibitor ADP ribosylates small GTP-binding proteins and induces hyperplasia of epidermis. J. Biol. Chem. **267:**2600–2604.
44. **Taylor, K. A., P. W. Luther, and M. S. Donnenberg.** 1999. Expression of the EspB protein of enteropathogenic Escherichia coli within HeLa cells affects stress fibers and cellular morphology. Infect. Immun. **67:**120–125.
45. **Vogel, L., and B. Baratte.** 1996. Suc1: cdc2 affinity reagent or essential cdk adaptor protein? Prog. Cell Cycle Res. **2:**129–135.
46. **Wachter, C., C. Beinke, M. Mattes, and M. A. Schmidt.** 1999. Insertion of EspD into epithelial target cell membranes by infecting enteropathogenic Escherichia coli. Mol. Microbiol. **31:**1695–1707.
47. **Waldman, T., C. Lengauer, K. W. Kinzler, and B. Vogelstein.** 1996. Uncoupling of S phase and mitosis induced by anticancer agents in cells lacking p21. Nature **381:**713–716.
48. **Warawa, J., B. B. Finlay, and B. Kenny.** 1999. Type III secretion-dependent hemolytic activity of enteropathogenic Escherichia coli. Infect. Immun. **67:** 5538–5540.
49. **Wolff, C., I. Nisan, E. Hanski, G. Frankel, and I. Rosenshine.** 1998. Protein translocation into host epithelial cells by infecting enteropathogenic Escherichia coli. Mol. Microbiol. **28:**143–155.

Editor: J. T. Barbieri